Electrochemical activity of *Geobacter sulfurreducens* biofilms on stainless steel anodes

Claire Dumas[a], Régine Basseguy[a] and Alain Bergel[a]

[a]Laboratoire de Génie Chimique CNRS-INPT, 5 rue Paulin Talabot, BP 1301, 31106 Toulouse Cedex 1, France

Abstract

Stainless steel was studied as anode for the biocatalysis of acetate oxidation by biofilms of *Geobacter sulfurreducens*. Electrodes were individually polarized at different potential in the range −0.20 V to +0.20 V vs. Ag/AgCl either in the same reactor or in different reactors containing acetate as electron donor and no electron acceptor except the working electrode. At +0.20 V vs. Ag/AgCl, the current increased after a 2-day lag period up to maximum current densities around 0.7 A m^{-2} and 2.4 A m^{-2} with 5 mM and 10 mM acetate, respectively. No current was obtained during chronoamperometry (CA) at potential values lower than 0.00 V vs. Ag/AgCl, while the cyclic voltammetries (CV) that were performed periodically always detected a fast electron transfer, with the oxidation starting around −0.25 V vs. Ag/AgCl. Epifluorescent microscopy showed that the current recorded by chronoamperometry was linked to the biofilm growth on the electrode surface, while CVs were more likely linked to the cells initially adsorbed from the inoculum. A model was proposed to explain the electrochemical behaviour of the biofilm, which appeared to be controlled by the pioneering adherent cells playing the role of "electrochemical gate" between the biofilm and the electrode surface.

Keywords : *Geobacter sulfurreducens*; Stainless steel; Biofilm; Electron transfer; Microbial fuel cell

1. Introduction

The recent discovery of bacteria that can transfer the electrons issued from their metabolism directly to solid anodes have created a new unexpected interest in microbial fuel cells (MFC) [1], [2], [3] and [4]. Different electrochemically active microbial species have been identified and several basic studies have been performed with pure cultures under constant potential chronoamperometry [5], [6] and [7]. The progressive attachment of the microbial cells onto the anode surface, which is most often polarised at +0.20 V vs. Ag/AgCl, has induced the increase of current density due to the oxidation of a soluble substrate, generally acetate or glucose, up to 0.07 A m^{-2}, 0.15 A m^{-2} and 0.25 A m^{-2} with *Rhodoferax ferrireducens* [8], *Desulfuromonas acetoxidans* [9] and *Geobacter metallireducens* [9] biofilms, respectively. *Geobacter*

sulfurreducens biofilms have given the highest current densities in the range 0.16–1.14 A m^{-2} on graphite anodes [6]. Cyclic voltammetry (CV) has also been performed to progress in the understanding of the microbial electrocatalysis mechanisms, but most of the studies investigated suspensions of microbial cells [7], [10], [11], [12] and [13] or freshly adherent micro-organisms [14]. CVs on mature biofilms has been more rarely reported [15]. Anodes are almost exclusively made of graphite, in some cases the surface modification with redox mediators have shown significantly increase of the electron transfer rate [16].
The purpose of this work was to contribute deciphering the electron transfer pathway and to assess the suitability of stainless steel as electrode material to support microbial anodes. It has already revealed very efficient to support microbial cathodes [17]. It is a well mastered industrial material, presents high mechanical properties, long-term resistance and is commercially available under many different compositions and morphologies. If it also revealed efficient to support microbial anodes, it would represent a promising solution to scale-up industrial microbial fuel cells.
To work in controlled conditions and to compare our results with previous data reported in literature on graphite electrodes, a similar experimental procedure than the one developed by Bond and Lovley was chosen: biofilms were grown with pure culture of *G. sulfurreducens* on anodes polarised at +0.20 V vs. Ag/AgCl [6]. The electrochemical reactors were filled with culture medium that did not contain any electron acceptor in order to force the cells to transfer the electrons they produce to the anode; acetate was used as the electron donor that underwent the microbially catalysed electrochemical oxidation. In the current state of the art, only a raw electrochemical scheme can be proposed to explain the biofilm-driven catalysis of acetate electrochemical oxidation, where acetate undergoes a metabolic oxidation, followed by direct transfer of the electrons from the microbial cells to the anode :

On the electrode surface:

(1)
$$\text{Cell(reduced)} \rightarrow \text{Cell(oxidised)} + m\, e^-$$

In the biofilm:

(2)
$$\text{Cell(oxidised)} + n CH_3COOH + 4n H_2O \rightarrow \text{Cell(reduced)} + 2n HCO_3^- + 10n H^+$$

2. Experimental

2.1. Media and growth conditions

G. sulfurreducens strain PCA (ATCC 51573) was obtained from DSMZ. Incubations were done at 30 °C during 5 days in the common growth medium already described elsewhere [6], which contained 50 mM sodium fumarate as electron acceptor and 10 mM acetate as electron donor. Unless otherwise stated, the electrochemical reactors were filled with the same medium, except that it lacked sodium fumarate. Reactors were flushed with a N_2/CO_2 (80–20%) stream during at

least 1 h, a lower flow was then maintained during the experiments. The electrochemical reactor was inoculated (5%, v/v) with cell suspensions that had an optical density at 620 nm around 0.3 (i.e. 142 000 CFU mL^{-1}).

2.2. Electrodes and electrochemical measurements

The body of the electrochemical reactor comprised two inlet and outlet ports and the top seven holes to set-up the electrodes and the gas flowing system. The junction between the top and the body of reactors was sealed with a clamping ring. Each working electrode, 1 cm × 2.5 cm × 0.1 cm pieces of stainless steel (UNS31254[1]), was drilled, tapped and a titanium wire was screwed on it. Before experiments, stainless steel coupons were cleaned with an ethanol/acetone (50–50%) mixture to dissolve organic adsorbed species, and with a fluoridric/nitric acids (2–20%) solution to dissolve the oxide layer. The platinum counter electrode (grid with 0.5 mm diameter wire) was cleaned by red-hot heating flame. Reference electrode was a silver/silver chloride wire. Its potential in the growth medium was around 0.31 V vs. SHE. All potential values are expressed with respect to this Ag/AgCl electrode throughout the paper.

One to four working electrodes (SS) were dipped in the same reactor and connected to the same auxiliary and reference electrodes through a multi-potentiostat (VMP1 or VMP2, software EC-Lab v.8.3, Bio-Logic SA). Each working electrode was individually polarized and the associated current registered thanks to a N-STAT device (Bio-Logic SA). Cyclic voltamogramms (CV) were recorded at 10 mV s^{-1} just before inoculation and then periodically during the experiment.

2.3. Microscopy and surface analysis

At the end of experiment, electrodes were removed from the reactor, stained with a solution of 0.03% orange acridine (A6014, Sigma) for 10 min, rinsed with distilled water and air dried in the dark. Pictures were taken with a Carl Zeiss Axiotech 100 microscope equipped for epifluorescence with HBO 50/ac mercury light source and Zeiss 09 filter (excitor AP 450–490, reflector FT 510, barrier filter LP 520). Image were acquired with a monochrome digital camera (Evolution VF) and post-treated with the software Image-Pro Plus v.5.

The average surface roughness (Ra) of the pre-treated electrodes was characterized using a white light interferometer Zygo New View 100 OMP-0348K.

3. Results

Four stainless steel electrodes were placed in the same reactor and polarised at −0.20 V, −0.10 V, +0.00 V and +0.20 V with respect to the same Ag/AgCl reference electrode. The reactor medium (2 L) contained 10 mM acetate but no electron acceptor. It was inoculated (5%, v/v) 1 h after the beginning of the polarization with a *G. sulfurreducens* suspension previously grown as described in Section 2. After around 2 days latency, the current density on the electrode polarised at +0.20 V started to increase and reached 2.4 A m^{-2} on day 7.6 (Fig. 1). Since this time, current density fell dramatically and remained at 0.1 A m^{-2} during the last 2 days. No current was recorded for the three other electrodes that were polarized at lower potential values (Fig. 1), indicating that the catalysis of the acetate oxidation could not occur at potential lower or equal to +0.00 V.

[1] Composition Cr, 19.9%; Ni, 17.8%; Mo, 6.0%; N, 0.2%; C, 0.01%; Fe, complement

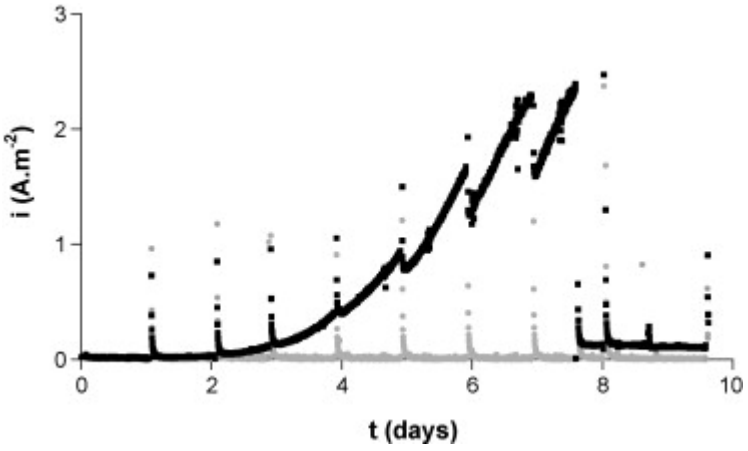

Fig. 1. Current density vs. time on stainless steel (experiment 1). Initial acetate concentration 10 mM, injection of bacteria 1 h after the beginning of polarization. (■) SS polarised at +0.20 V vs. Ag/AgCl. (▰) SS1.2 polarised at −0.10 V vs. Ag/AgCl. Perturbation in current every 24 h were due to CV recordings.

CVs were performed at 10 mV s^{-1} just before and just after inoculation and then every 24 h on each electrode during chronoamperometry. CV recordings disturbed the current transiently but it recovered rapidly its value after a few minutes back under constant polarization. CVs recorded before and just after the inoculum injection were flat, indicating that no redox process occurred. Then all CVs exhibited exactly the same general shape, whatever the imposed potential value during the chronoamperometry, with a clear reduction process and a flat oxidation wave (Fig. 2). The maximum of the oxidation wave occurred between 0.05 V and 0.12 V with similar current density values. For instance, at day 7.6 current densities were 10.2 A m^{-2}, 12.0 A m^{-2}, 9.7 A m^{-2} and 10.5 A m^{-2} for the electrode polarised at +0.20 V, +0.00 V, −0.10 V and −0.20 V, respectively. The potential of inversion between reduction and oxidation was also very stable around −0.25 V. CVs did not exhibit any significant difference with respect to the potential imposed during chronoamperometry. In order to follow the evolution in CVs as a function of time, the current densities obtained daily on the CVs at +0.20 V are reported in Fig. 3. No oxidation was detected just after injecting the inoculum, but the CV oxidation current increased quickly close to its maximal value since the first day and kept high values until the end of the experiment. CVs did not reproduce the exponential current increase that was observed during chronoamperometry from day 2 to day 7, and they were also not sensitive to the drastic perturbation observed at day 7 on the chronoamperometry. It can be concluded that CV and chronoamperometry addressed different phenomena.

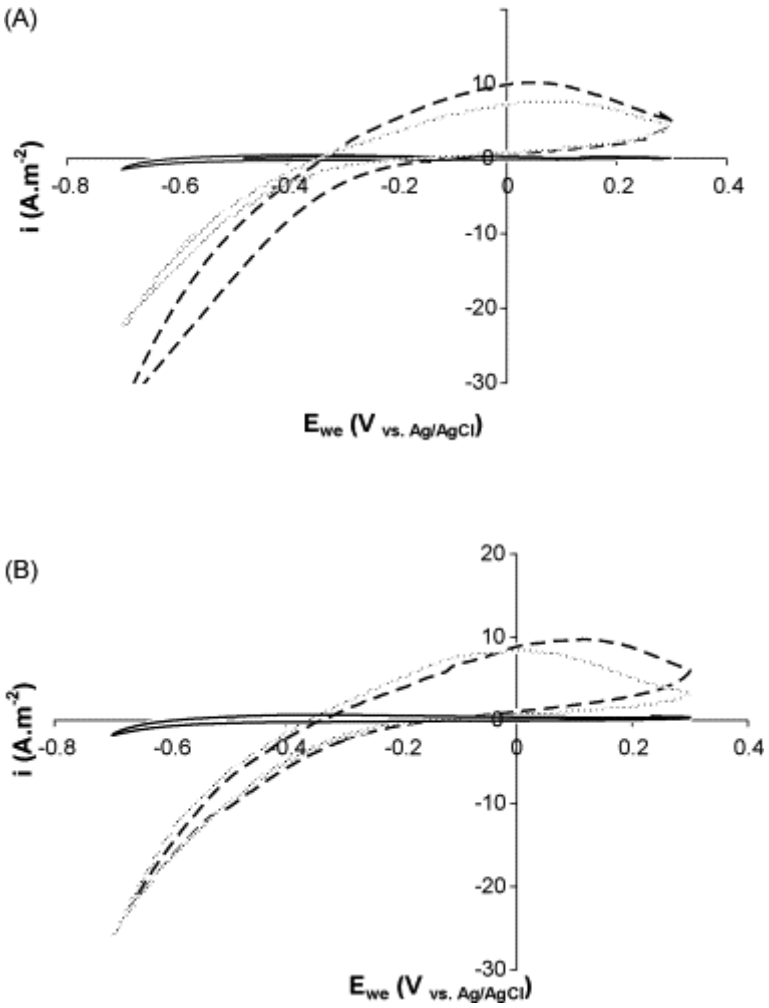

Fig. 2. Evolution of CVs (10 mV s^{-1}) on stainless steel electrode (experiment 1): ( ) day 2.9, (- - -) day 7.6, (—) at the end of the experiment after biofilm removal with the cleaned electrode back in the reactor. (A) Electrode polarised at +0.20 V vs. Ag/AgCl. (B) Electrode polarised at −0.10 V vs. Ag/AgCl.

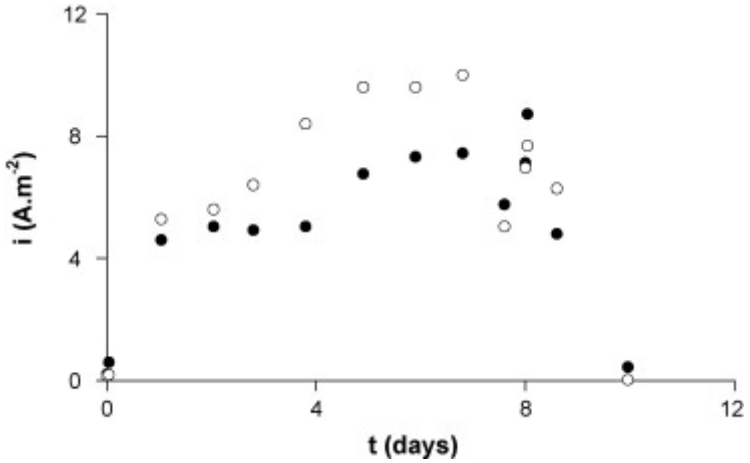

Fig. 3. Evolution of the current density at +0.20 V vs. Ag/AgCl from the CVs performed during experiment 1 (●) on the electrode polarized at −0.10 V vs. Ag/AgCl and (○) on the electrode polarized at +0.20 V vs. Ag/AgCl. Last values were recorded after biofilm removal.

At the end of the experiment, the biofilm was removed from the electrode surface by gentle mechanical cleaning and the electrode was set back into the reactor to perform the final CV (Fig. 2A and B). When biofilm was removed from the electrode, the CV recorded with the cleaned electrode that was put back in the reactor was exactly similar to the initial CV performed before inoculation (Fig. 2). The biofilm was consequently fully responsible for the reduction and oxidation processes, as it has been previously established in similar conditions with graphite electrodes [6].

At the end of the experiment, epifluorescence microscopy pictures were taken on each electrode surface on several randomly chosen spots. The pictures reported here were representative of the biofilm spreading out (Fig. 4). On the electrode polarised at +0.20 V (Fig. 4A), the biofilm was dense and distributed all over the electrode surface. It recovered around 57 ± 8% of the electrode surface while the biofilm coverage ratio was around 39 ± 6% when the initial acetate concentration was equal to 5 mM. On the electrodes polarised at lower potentials (Fig. 4B and C), there were only scattered bacteria or a few small clusters on the electrode surface. The biofilm covered around 12 ± 2% (Fig. 4B), 15. ± 7 (Fig. 4C), 15 ± 9% (Fig. 4D). On the electrode polarised at −0.20 V, a few large clusters were noticed, as depicted in Fig. 4D, but the biofilm was never covering the entire electrode surface like on an electrode polarised at +0.20 V. The clear difference between the biofilm morphology on the electrode polarized at +0.20 V and the others was consistent with the behaviour of the electrode during chronoamperometry, as only the fully covered electrode supplied current in chronoamperometry. On the contrary, CVs seemed not to be straightforwardly linked to the biofilm coverage since even on the electrodes colonised by a few bacteria, high current densities were detected on CVs.

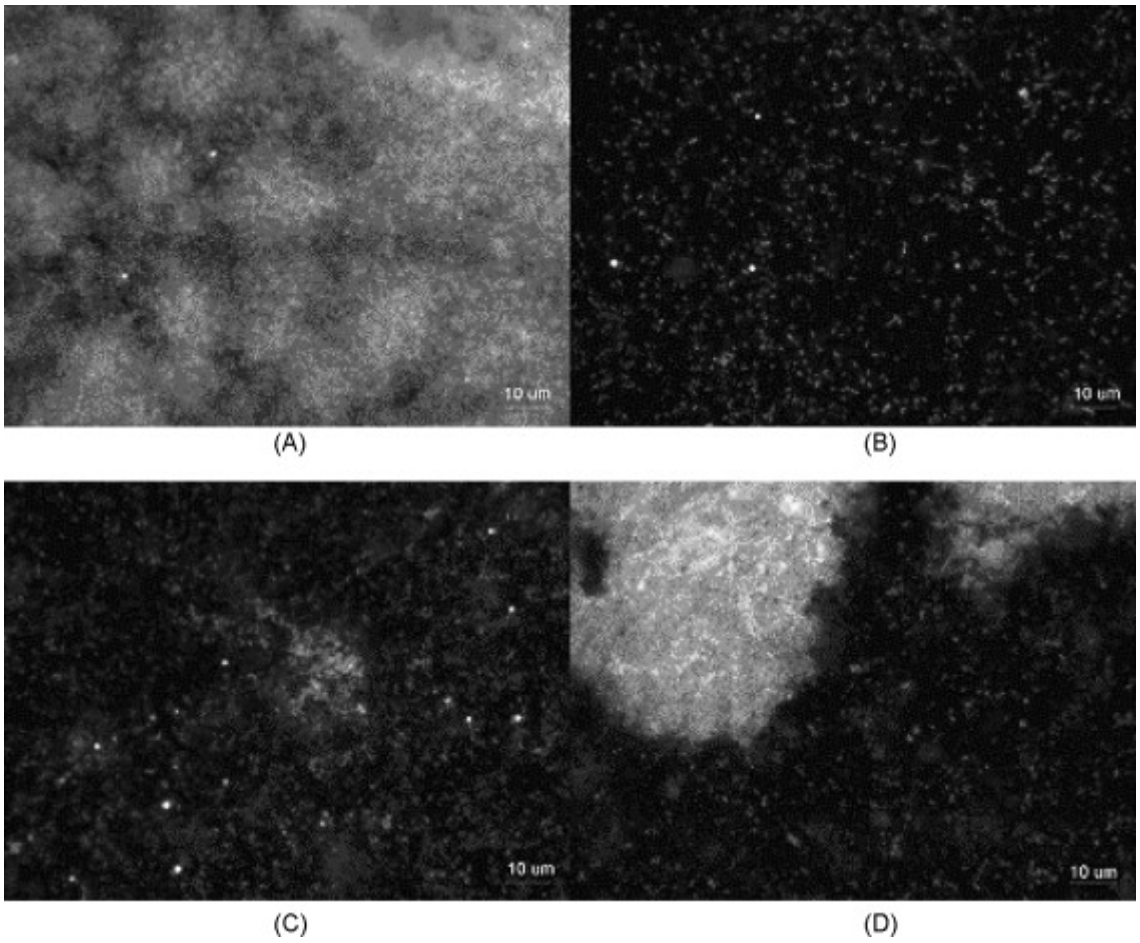

Fig. 4. Epifluorescent microscopy of the electrodes at the end of experiment 1; polarization at (A) +0.20 V vs. Ag/AgCl; (B) −0.10 V vs. Ag/AgCl; (C) 0.00 V vs. Ag/AgCl; (D) −0.20 V vs. Ag/AgCl.

As all electrodes were dipped in the same reactor in experiment 1, it might be suspected that the microbial cells observed on the surface of the electrodes that were polarized at low potential values may result from cells that were released from the well-developed biofilm growing on the electrode polarized at +0.20 V. In order to check this assumption the experiment was repeated with four separated reactors in parallel, each containing only one electrode (experiment 2). Each electrochemical reactor contained 0.5 L medium with 5 mM acetate and were inoculated at day 0.8 (i.e. 19 h after starting polarization) with 5% (v/v) of the same *G. sulfurreducens* culture. The potential was imposed from the beginning of the experiment and was then changed on day 8.9:

- Electrode A: was kept at +0.20 V the whole experiment long;
- Electrode B: initially at +0.20 V, was set at 0.00 V at day 8.9;
- Electrode C: initially at −0.20 V was set at +0.20 V at day 8.9;
- Electrode D: initially at 0.00 V was set at +0.20 V at day 8.9.

Electrodes A and B polarized at +0.20 V (Fig. 5A and B) showed similar behaviours: the current density started to increase around 2 days after inoculation (i.e. on day 3) and reached 0.4 A m^{-2} and 0.3 A m^{-2} on day 8.9 for electrodes A and B, respectively. As soon as the potential of

electrode B was changed (day 8.9), from +0.20 V to +0.00 V, the current density went down to zero, while electrode A that was kept +0.20 V continued slowly to increase up to 0.7 A m^{-2} on day 19.5. As was observed in experiment 1, electrodes C and D polarized at −0.20 V and +0.00 V gave no current (Fig. 5C and D). One day after the change in potential to +0.20 V, current density increased and reached for both electrodes (C and D) approximately 0.5 A m^{-2} on day 19.5.

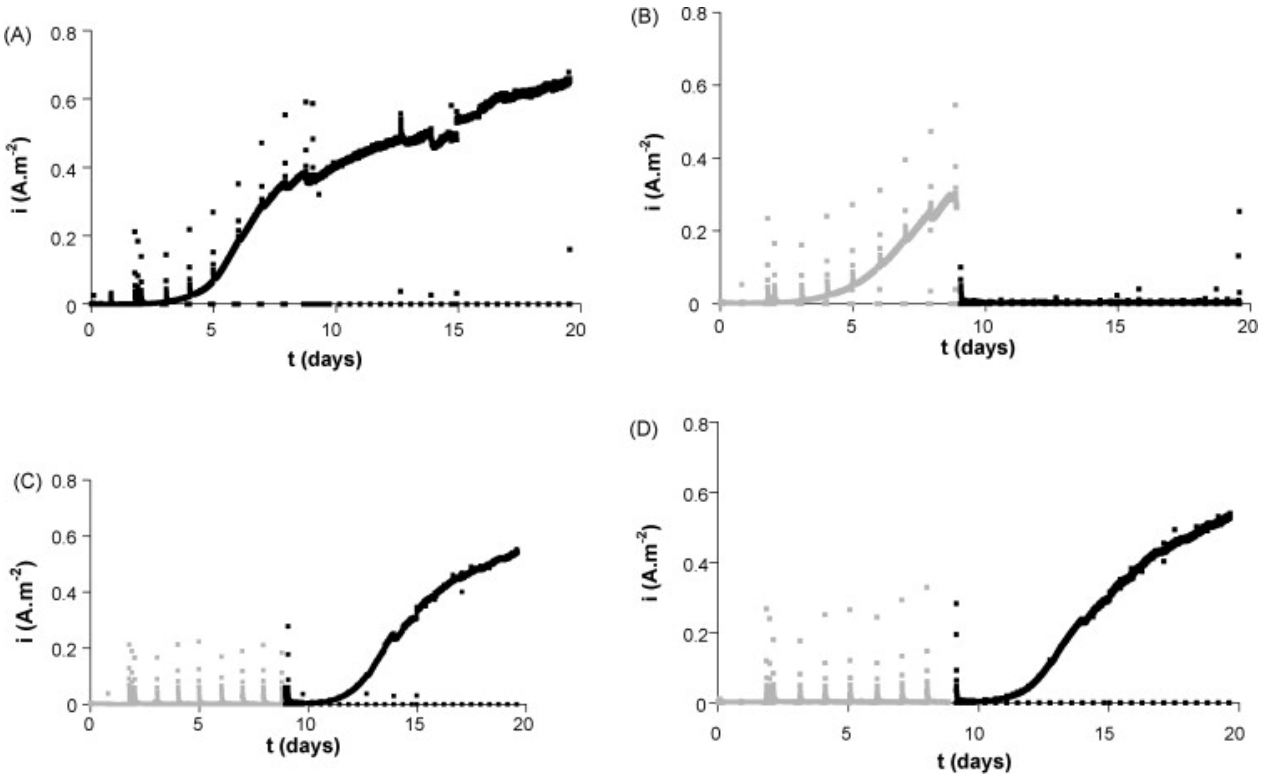

Fig. 5. Current density vs. time on stainless steel electrode (experiment 2). Initial acetate concentration 5 mM, injection of bacteria on day 0.8 (19 h). (A) Electrode polarised at +0.20 V vs. Ag/AgCl; (B) polarised at +0.20 V vs. Ag/AgCl from day 0 to day 8.9, then at +0.00 V vs. Ag/AgCl to the end; (C) polarised at −0.20 V vs. Ag/AgCl from day 0 to day 8.9, then at +0.20 V vs. Ag/AgCl to the end; (D) polarised at +0.00 V vs. Ag/AgCl from day 0 to day 8.9, then at +0.20 V vs. Ag/AgCl to the end.

The CVs performed on the fourth electrodes on day 8.9 before the change in potential were similar to the CVs recorded in experiment 1. A similar flat oxidation wave appeared even with electrodes C and D polarised at low potential values that did not supply any current. At day 8.9, just before the potential change, the current densities recorded at +0.20 V vs. Ag/AgCl on the CVs were 7.7 A m^{-2}, 7.0 A m^{-2}, 7.6 A m^{-2} and 8.4 A m^{-2} for electrodes A, B, C and D, respectively. The potential change did not affect these values significantly. When biofilm was removed, the current always went to zero confirming the essential role of biofilm in the oxidation and reduction reactions.

A third experiment was carried out independently in a 0.5 L reactor with 10 mM acetate and only one stainless steel electrode polarised at +0.20 V. Inoculation was made at day 4.8. The current density increased since day 6.8 (2 days after inoculation) and reached a maximum value of 1.1 A m^{-2} on day 12.6 (Fig. 6). The CV exhibited the same shape as previously but with lower current densities, around 2 A m^{-2} at +0.20 V. At day 13.1 the reactor was purged, keeping it under N_2/CO_2 atmosphere. It was then refilled with fresh medium always containing 10 mM acetate. The current was slightly disturbed by the change of medium but returned to a value of 0.8 A m^{-2} after around 20 h, which remained stable for days. The current was a little bit lower than the value before medium removal, even if electrode was kept under N_2/CO_2 atmosphere, the biofilm was probably affected by the drain of the reactor. As it has already been demonstrated with graphite electrode [6], it was confirmed that the catalysis of acetate oxidation was not linked to the production of a compound that would accumulate in solution.

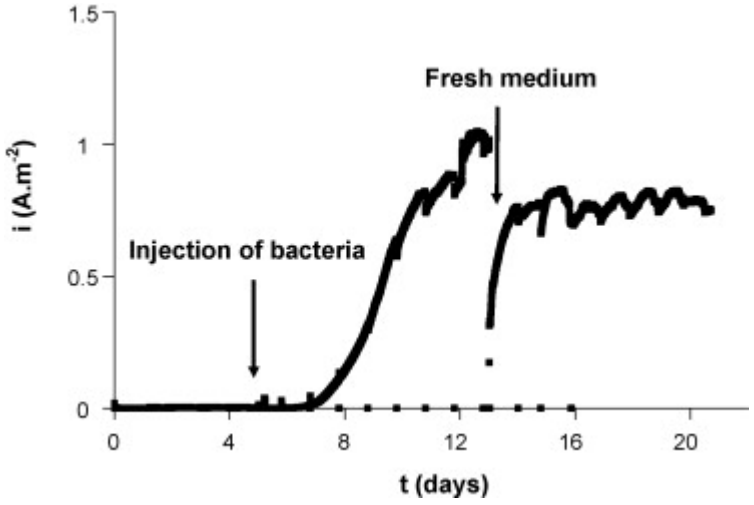

Fig. 6. Evolution of the current density on stainless steel polarised at +0.20 V vs. Ag/AgCl with 10 mM acetate (experiment 3). The inoculation was made at day 4.8 and the medium was replaced with fresh medium on day 13.1.

4. Discussion

It is now well established that biofilms of *G. sulfurreducens* are able to catalyse the oxidation of acetate transferring directly the electrons to graphite anodes [6]. CVs performed when the biofilm was removed from the electrode surface (experiments 1 and 2) and chronoamperometry after renewing the medium (experiment 3) both confirmed that the biofilm was fully responsible for the catalysis of acetate oxidation. Neither planktonic cells nor products that would accumulate in the bulk were involved in the process.

The epifluorescent microscopy pictures confirmed that the current supply in chronamperometry was linked to the formation of a well-developed biofilm (Fig. 4A). On the contrary, potential values lower or equal to 0.00 V vs. Ag/AgCl did not result in current supply and the electrodes exhibited only a very low colonization (Fig. 4B–D). Experiment 1, in which all electrodes were

dipped in the same reactor, indicated obviously that the difference cannot be attributed to discrepancy in the biological conditions, but only to the value of the applied potential. Similarly, it has already been observed that more positive anode potential favours colonization by electrode-reducing micro-organisms [14]. The effect of the potential has also been shown on the colonization of graphite anodes by *Shewanella oneidensis MR-1* [18], both on the initial lag time and the maximum current.

Surprisingly, whenever the electrode was polarised at +0.20 V, since the beginning of the experiment (Fig. 5A and B) or several days after inoculation (Fig. 5C and D), the current increased in the same manner: a lag time of 1 or 2 days followed by a sharp increase. Actually, the bacteria inoculated in the medium at day 0.8 in experiment 2 survived during more than 8 days before the potential was changed, although they cannot use the electrode as electron acceptor. Colonization from other electrodes cannot be evoked in experiment 2, as the four reactors were independent. It may be thought that traces of fumarate remaining in the inoculum could enable bacteria to survive during a few days. The presence of remaining organic acids in the medium due to inoculum has already been reported [19]. It may also be assumed that potential in the range −0.20 V to 0.00 V may be sufficient for the bacteria to survive on the electrode surface, but not to grow on it.

Under chronoamperometry the maximum current density obtained was around 2.4 A m^{-2} (experiment 1) and 1.0 A m^{-2} (experiment 3) with 10 mM acetate, while less than 0.7 A m^{-2} was reached with 5 mM acetate (experiment 2). It may be concluded that acetate concentration have a direct effect on bacterial electricity production. This general behaviour was consistent with the data reported elsewhere. Increasing the lactate concentration above 5 mM has been shown to decrease the lag time and to increase the peak of current obtained with *Shewanella oneidensis MR-1* [18]. *G. sulfurreducens* has given current density around 0.5 A m^{-2} on a graphite electrode maintained at +0.20 V vs. Ag/AgCl with acetate at or below 2 mM, and the current rose up to 1.1 A m^{-2} with 10 mM [6]. Under +0.52 V vs. SHE, *Geopsychrobacter electrodiphilus* [20] have sustained 88.9 A m^{-2} for the reduction of 2 mM fumarate and the current density reached 1214.3 A m^{-2} with 10 mM. These results evidenced the importance of substrate concentration in current production, even if a straightforward relationship cannot be evoked. Nevertheless, this conclusion should be qualified as the experiments reported in the literature have rarely been repeated in the same conditions to get a really sure relationship. For instance, experiments that were repeated here in similar conditions (data not shown) revealed an opposite behaviour with current densities of 0.55 A m^{-2} with 10 mM acetate and 1.6 A m^{-2} with 5 mM. Actually, other parameters like the ratio of the number of cells inoculated with respect to the electrode surface area, and mainly the biological quality of the strain, linked for instance to the number of replicates, may have an important effect. It was also observed that acetate has a drastic inhibiting effect on the current at concentration of 50 mM (data not shown).

In identical experimental conditions (inoculation of *G. sulfurreducens*, imposed potential +0.20 V vs. Ag/AgCl, 5 mM acetate in the medium) we have found in previous experiments current densities around 8.0 A m^{-2} and 5.0 A m^{-2} with graphite and dimensionally stable anodes (DSA®), respectively [21]. These values have appeared to be directly correlated to the average surface roughness of the materials of 5.6 μm and 3.2 μm for graphite and DSA, respectively. The average roughness of stainless steel electrode was measured here close to 0.29 μm. Flint et al. claimed that bacterial adhesion is favoured by entrapment on material surfaces that present surface roughness close to the size of microbial cells [22]. It might be expected that the results might be improved by increasing the surface roughness, as the average value of 0.29 μm was significantly less than the size of a microbial cell.

CV obviously addressed a different phenomenon than chronoamperometry. CVs were not sensitive to the potential applied during chronoamperometry. They gave the same results with the electrodes colonized by small scattered colonies than with the fully developed biofilm. They exhibited very high currents since the first day after inoculation and did not reproduce the exponential current increase observed in chronoamperometry. The currents recorded by CV did not depend on the concentration of acetate. CVs were not sensitive to the event that provoked the drastic current drop observed on the seventh day in experiment 1: the chronoamperometry did no longer supply any current, while CVs were not affected. Finally, the most surprising difference may be that CV always indicated that the oxidation process started around −0.25 V, while chronoamperometries at −0.20 V, −0.10 V and 0.00 V gave absolutely no current.

It may be concluded that CV addressed adherent cells that are able to exchange electrons with the electrode. This transfer is fast with a redox potential around −0.25 V. The number of cells that are able to achieve this electron transfer did not vary in a large extend during the experiment since the first day after inoculation. These cells or small colonies should consequently mainly result from adhesion of cells contained in the inoculum. So it was sufficient for these cells to survive on the electrode surface to maintain the high currents recorded during CV. These high currents may be due to the fast charge/discharge of the electrons that were stored in the adherent cells :

(3)
Cell(0) ? Cell(+1)+e− ⇔…… ⇔ Cell($N_{threshold}$)+e− ⇔ …… ⇔Cell(N)+e−

and they do not require the full activity of the metabolic pathways. Even when the full metabolism of acetate oxidation was active at +0.20 V, CV at 10 mV s^{-1} were not affected by the metabolic process, which corresponded to a too low time-scale with respect to the fast direct electron exchange (Eq. (3)). The absence of the oxidation of acetate at low potential values during chronoamperometry suggests that the cells can drive this reaction only when they get a redox state (N) high enough ($N > N_{threshold}$). Eqs. (1) and (2) should thus be written :

(4)
Cell($N_{threshold}$)⇔Cell(N)+me^- fast

(5)
Cell(N) + $n$$CH_3COOH$ + 4$n$$H_2O$ → Cell($N_{threshold}$) + 2$n$$HCO_3^-$ + 10$n$$H^+$ slow

It has been demonstrated elsewhere that the *Geobacter*-catalysed oxidation of acetate can occur at slightly lower potential values around 0.05 V vs. Ag/AgCl on DSA and graphite anodes [21]. This potential threshold remained far from the redox potential of acetate oxidation to CO_2 $E_{acetate/CO2}°$ of −0.29 V vs. SHE [23], i.e. −0.60 V vs. Ag/AgCl in the experimental conditions used here. This is consistent with the recent suggestion that the microbial cells need a significant portion of potential energy liberated from oxidation of acetate for their own metabolic benefit [24].

Under constant potential at +0.20 V, the redox state of the adherent cells was high enough to activate the metabolic pathways and the biofilm developed around them. These cells play thus the role of "electrochemical gates" between the electrode surface and the biofilm. The others cells were not able to exchange directly electrons with the electrode surface, otherwise the current recorded by CV would increase according to the biofilm development. This scheme is consistent with the two different electron transfer pathways that have been distinguished in the literature. Direct electron exchange with the electrode surface have been demonstrated to be carried out through outer-membrane cytochromes [25]. This mechanism obviously requires adhesion of the cell on the electrode surface. In addition, pili that constitute conductive nanowires have been identified in the biofilms that supplied the higher currents [26] and [27]. These pili have been believed to ensure electric connection from cell to cell, whereas they seemed not to be involved in the direct electron transfer to the electrode surface [25]. Here, such a kind of electrochemical connection may be assumed between the pioneering adherent cells and the cells growing then around them. The scheme is also consistent with the global aspect of the fully developed biofilms observed on the electrodes polarised at 0.20 V. The clear structure into circles of around 20 μm diameter (Fig. 4A) nicely supports an organisation into clusters around the electrochemical gate cells.

Finally, it must be noted that a clear difference occurred between the electrochemical behaviour of the biofilms formed here on stainless steel, and similar biofilms formed previously on graphite and DSA anodes [21]. On graphite and DSA, CVs recorded during chronoamperometry followed the evolution of the chronoamperometry. It means that the oxidation peak started on CV around the same potential value as with chronoamperometry (around 0.05 V vs. Ag/AgCl) and the current recorded by CV increased as a function of time, with a proportional relationship with the current obtained under chronoamperometry. The behaviour revealed here was thus related to specific features of the initial adsorption of the cells on stainless steel surface.

5. Conclusions

The general aim of the work in progress in the laboratory consists in defining optimal materials that could be used in large scale MFC for long-term operation. In this framework, stainless steel was checked here because of its large industrial availability, mechanical properties, long-term resistance to corrosion and reasonable cost. It gave here lower current densities than graphite or DSA checked previously in identical conditions, but the lower average surface roughness might be detrimental to the stainless steel electrodes checked here. Comparing chronoamperometry, cyclic voltammetry, surface coverage ratios and biofilm morphology led to propose a model for the electron transfer that underlined the role of "electrochemical gate" played by the first adherent cells. It seems that cell adhesion that took place in the first hours controlled in a large extend the further electron transfer process. The electrochemical efficiency of the stainless steel/biofilm interface might consequently be improved by optimising the initial adhesion of pioneering cells on the electrode surface.

Acknowledgments

This work was financially supported by the Sixth Framework Program of the European Union as part of the project “Electrochemically Active Biofilms” NEST (508866). The authors are most grateful for technical contributions from Luc Etcheverry, engineer CNRS, Laboratoire de Génie Chimique (Toulouse, France).

References

[1] D.R. Lovley, *Microbe* **1** (2006), p. 323.

[2] D.R. Lovley, *Nat. Rev. Microbiol.* **4** (2006), p. 499.

[3] B.E. Logan, B. Hamelers, R. Rozendal, U. Schroder, J. Keller, S. Freguia, P. Aelterman, W. Verstraete and K. Rabaey, *Environ. Sci. Technol.* **40** (2006), p. 5181.

[4] K. Rabaey and W. Verstraete, *Trends Biotechnol.* **23** (2005), p. 291.

[5] B.H. Kim, H.J. Kim, M.S. Hyun and D.H. Park, *J. Microb. Biotechnol.* **9** (1999), p. 127.

[6] D.R. Bond and D.R. Lovley, *Appl. Environ. Microbiol.* **69** (2003), p. 1548.

[7] S.A. Lee, Y. Choi, S. Jung and S. Kim, *Bioelectrochemistry* **57** (2002), p. 173.

[8] S.K. Chaudhuri and D.R. Lovley, *Nat. Biotechnol.* **21** (2003), p. 1229.

[9] D.R. Bond, D.E. Holmes, L.M. Tender and D.R. Lovley, *Science* **295** (2002), p. 483.

[10] H.S. Park, B.H. Kim, H.S. Kim, H.J. Kim, G.T. Kim, M. Kim, I.S. Chang, Y.K. Park and H.I. Chang, *Anaerobe* **7** (2001), p. 297.

[11] C.A. Pham, S.J. Jung, N.T. Phung, J. Lee, I.S. Chang, B.H. Kim, H. Yi and J. Chun, *FEMS Microbiol. Lett.* **223** (2003), p. 129.

[12] K. Rabaey, N. Boon, M. Hofte and W. Verstraete, *Environ. Sci. Technol.* **39** (2005), p. 3401.

[13] Y. Choi, E. Jung, S. Kim and S. Jung, *Bioelectrochemistry* **59** (2003), p. 121.

[14] K. Rabaey, N. Boon, S.D. Siciliano, M. Verhaege and W. Verstraete, *Appl. Environ. Microbiol.* **70** (2004), p. 5373.

[15] H. Liu, S. Cheng and B.E. Logan, *Environ. Sci. Technol.* **39** (2005), p. 658.

[16] D.A. Lowy, L.M. Tender, J.G. Zeikus, D.H. Park and D.R. Lovley, *Biosens. Bioelectron.* **21** (2006), p. 2058.

[17] C. Dumas, R. Basséguy and A. Bergel, *Electrochim. Acta* **53** (2008), p. 2494.

[18] E.J. Cho and A.D. Ellington, *Bioelectrochemistry* **70** (2007), p. 165.

[19] K.B. Gregory, D.R. Bond and D.R. Lovley, *Environ. Microbiol.* **6** (2004), p. 596.

[20] D.E. Holmes, J.S. Nicoll, D.R. Bond and D.R. Lovley, *Appl. Environ. Microbiol.* **70** (2004), p. 6023.

[21] C. Dumas, R. Basséguy and A. Bergel, *Electrochim. Acta* **53** (2008), p. 3200.

[22] S.H. Flint, J.D. Brooks and P.J. Bremer, *J. Food Eng.* **43** (2000), p. 235.

[23] R.K. Thauer, K. Junkermann and K. Decker, *Bacteriol. Rev.* (1977), p. 100.

[24] D.A. Finkelstein, L.M. Tender and J.G. Zeikus, *Environ. Sci. Technol.* **40** (2006), p. 6990.

[25] D.E. Holmes, S.K. Chaudhuri, K.P. Nevin, T. Mehta, B.A. Methé, A. Liu, J.E. Ward, T.L. Woodard, J. Webster and D.R. Lovley, *Environ. Microbiol.* **8** (2006), p. 1805.

[26] G. Reguera, K.D. McCarthy, T. Mehta, J.S. Nicoll, M.T. Tuominen and D.R. Lovley, *Nature* **435** (2005), p. 1098.

[27] Y.A. Gorby, S. Yanina, J.S. McLean, K.M. Rosso, D. Moyles, A. Dohnalkova, T.J. Beveridge, I.S. Chang, B.H. Kim, K.S. Kim, D.E. Culley, S.B. Reed, M.F. Romine, D.A. Saffarini, E.A. Hill, L. Shi, D.A. Elias, D.W. Kennedy, G. Pinchuk, K. Watanabe, S.I. Ishii, B. Logan, K.H. Nealson and J.K. Fredrickson, *Proc. Natl. Acad. Sci. U.S.A.* **103** (2006), p. 11358.

Published in :

Electrochimica Acta
Volume 53, Issue 16, 30 June 2008, Pages 5235-5241